Dedicated to innovation in aerospace

NLR-TP-2020-160 | April 2020

Korean Utility Helicopter KUH-1 Icing Certification Program

CUSTOMER: Royal Netherlands Aerospace Centre

NLR – Royal Netherlands Aerospace Centre

Dedicated to innovation in aerospace

Korean Utility Helicopter KUH-1 Icing Certification Program

REPORT NUMBER
NLR-TP-2020-160

AUTHOR(S)
S.C. van 't Hoff
K.H. Lammers
Y.S. Hwang
J.S. Kim
K.S. Kim

REPORT CLASSIFICATION
UNCLASSIFIED

DATE
April 2020

KNOWLEDGE AREA(S)
Helicopter Technology

DESCRIPTOR(S)
Helicopter
icing
KUH

Problem area

This report provides an overview of the icing qualification program of the Korean Utility Helicopter (KUH) and a description of the most recent KAI-NLR design and test activities related to key ice protection systems.

Description of work

The KAI-NLR test activities performed include 1) component-level development and qualification icing wind tunnel testing at Cox & Co in Long Island, NY, 2) icing qualification testing of the engine air intake ice protection system at Rail Tec Arsenal (RTA) in Vienna, Austria, 3) artificial icing flight testing using the US Army Helicopter Icing Spray System (HISS), and 4) natural icing flight testing of the complete aircraft in the state of Michigan, USA.

Results and conclusions

Under the pressure of an ambitious delivery schedule, the KUH-1 icing qualification program has seen a large number of test activities over a relatively short period of roughly three years. Despite the aggressive development schedule, the hard work and collaboration of all parties involved has led to a successful conclusion to the KUH-1 icing qualification in July of 2018.

Applicability

The ice protection system design and test activities described herein are applicable to helicopter qualification for flight in icing conditions.

GENERAL NOTE
This report is based on a presentation held at the 2019 SAE International Icing Conference, Minneapolis, 18-21 June 2019.

NLR
Anthony Fokkerweg 2
1059 CM Amsterdam, The Netherlands
p) +31 88 511 3113
e) info@nlr.nl i) www.nlr.nl

Dedicated to innovation in aerospace

NLR-TP-2020-160 | April 2020

Korean Utility Helicopter KUH-1 Icing Certification Program

CUSTOMER: Royal Netherlands Aerospace Centre

AUTHOR(S):

S.C. van 't Hoff	NLR
K.H. Lammers	NLR
Y.S. Hwang	KAI
J.S. Kim	KAI
K.S. Kim	KAI

NLR – Royal Netherlands Aerospace Centre

This report is based on a presentation held at the 2019 SAE International Icing Conference, Minneapolis, 18-21 June 2019.

CUSTOMER	**Royal Netherlands Aerospace Centre**
CONTRACT NUMBER	**-----**
OWNER	**NLR**
DIVISION NLR	**Aerospace Vehicles**
DISTRIBUTION	**Unlimited**
CLASSIFICATION OF TITLE	**UNCLASSIFIED**

APPROVED BY:		**Date**
AUTHOR	S.C. van 't Hoff	14-04-2020
REVIEWER	K.H. Lammers	15-04-2020
MANAGING DEPARTMENT	J.F. Hakkaart	15-04-2020

Summary

The KUH-1 Surion is a twin-engine utility helicopter designed and developed jointly by Korea Aerospace Industries (KAI) and Airbus Helicopters primarily for the Republic of Korea Army (ROKA). Following customer requirements, KAI launched a program aimed at the military qualification of the KUH-1 for flight in icing conditions following tailored airworthiness certification criteria based on 14 CFR Part 29 and DEF STAN 00-970.

The Netherlands Aerospace Centre (NLR) became involved in the program on the eve of the first icing flight test campaign performed in the winter of 2015/2016. NLR has supported all subsequent test activities and the finding of compliance in close collaboration with KAI and certain suppliers. The test activities performed include 1) component-level development and qualification icing wind tunnel testing at Cox & Co in Long Island, NY, 2) icing qualification testing of the engine air intake ice protection system at Rail Tec Arsenal (RTA) in Vienna, Austria, 3) artificial icing flight testing using the US Army Helicopter Icing Spray System (HISS), and 4) natural icing flight testing of the complete aircraft in the state of Michigan, USA.

Following the extensive test activities, the KUH-1 was granted icing qualification by the Korean military airworthiness authorities in June of 2018. This report provides an overview of the KUH-1 icing certification program, followed by a more detailed accounting of the most recent icing wind tunnel and flight test activities as outlined above, and a description of the ice protection system design for the engine air intake, the upper wire cutter and the main rotor system.

Contents

Abbreviations

ACRONYM	DESCRIPTION
CCP	Cloud Combination Probe
CFD	Computational Fluid Dynamics
CMI	Continuous Maximum Icing
HISS	Helicopter Icing Spray System
IDS	Ice Detection System
IPS	Ice Protection System
IRMP	Ice Rate Meter Panel
IWT	Icing Wind Tunnel
KHP	Korean Helicopter Program
LWC	Liquid Water Content
MVD	Median Volume Diameter
NLR	Royal Netherlands Aerospace Centre
NR	Rotor Speed
OAT	Outside Air Temperature
RIPS	Rotor Ice Protection System
PMI	Periodic Maximum Icing
ROKA	Republic of Korea Army
SLD	Supercooled Large Drops
UTC	Universal Coordinated Time
VNE	Never Exceed Speed
VY	Best-Climb Speed

1 Introduction

The capability to operate in icing conditions greatly improves operational availability, particularly near large bodies of water in regions with relatively harsh winters such as the Northern United States and Canada, as well as the Korean peninsula. All-weather capability is especially important for offshore transport, Search and Rescue, and littoral military operations. For this reason, the qualification of the KUH-1 for flight in icing conditions is crucial to maximize the utility of the aircraft for the ROKA and other future operators.

The development of the KUH-1 ice protection system initially saw the integration of existing technologies previously proven on aircraft like the Sikorsky UH-60 and the Airbus AS332. However, despite the use of existing technical solutions, several systems were redesigned to improve performance and meet the installation and icing requirements specific to the KUH-1. A different approach was taken for the engine air intake, where KAI opted for the in-house development of an aerodynamically efficient electrothermal anti-icing solution to be able to meet the stipulated performance requirements for the clean aircraft with ice protection systems installed. This design choice subsequently led to a requirement to anti-ice the upper wire cutter which is located in close proximity to the engine air intakes. An integrated coil-heater design was selected as a cost-effective solution that could be implemented without impacting the wire strike qualification.

In advance of the first icing flight test campaign in 2015/2016 [1], KAI initiated a numerical icing analysis effort of the various serial production subsystems to predict their performance and identify the critical icing conditions. Based on the results of this exercise, backup flight test configurations were prepared for both the engine air intake and main rotor IPS. In addition, simulated ice shape flight tests were performed to demonstrate the (negligible) impact of horizontal stabilizer ice accretion on aircraft stability. The 2015/2016 artificial and natural icing flight testing revealed a number of remaining deficiencies that were addressed in a subsequent effort.

The continued development of the engine air intake and wire cutter ice protection systems was supported by 3-D drop impingement and 2-D thermal analyses performed by KAI and AeroTex UK [2], as well as KAI-NLR 2-D icing wind tunnel testing performed at Cox & Co, and full-scale testing of the prototype engine intake at RTA [4]. Relying on hardware previously certificated on the AS332, the modifications to the main rotor IPS focused on the deicing logic, with the principal aim to reduce the average icing torque rise and meet the ROKA performance requirements.

This report provides an overview of the KUH-1 icing qualification program and a description of the most recent KAI-NLR design and test activities related to key ice protection systems. A chronological overview of the icing test activities since the first flight test campaign is provided in Figure 1.

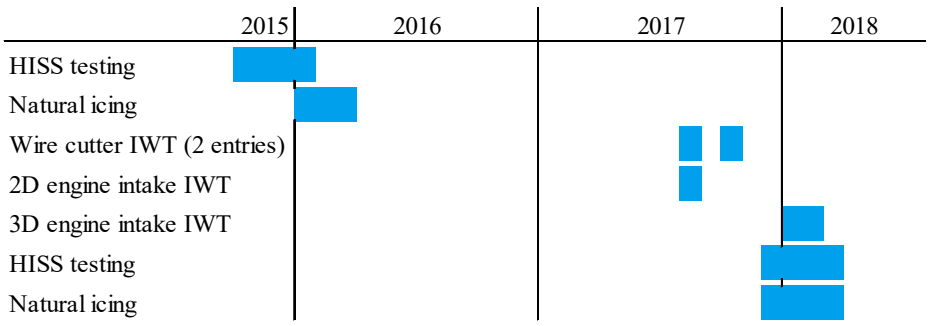

Figure 1: Overview of test history for KUH-1 icing qualification, starting with the first icing flight test campaign.

2 Engine air intake ice protection

2.1 Design description

The KUH-1 is qualified for flight in icing conditions without engine air intake screens or barrier filters installed. Ice protection of the engine induction system is achieved through an electrothermal heater, the extent of which is shown in Figure 2. In the direct vicinity of the engine inlet, the heater is assisted by the engine bleed air anti-icing of the T700 engines installed on the aircraft. The electrical power budget available from the two generators necessitates a running-wet anti-icing design with a power density distribution tailored to minimize runback ice accretion.

To minimize the formation of runback ice aft of the anti-iced area, the power density distribution of the KUH-1 engine intake heater mat has been fine-tuned over multiple design and test iterations. The highest power density area is located from the stagnation line towards the outer edge of the intake, where the protected extent is constrained by the presence of the engine bay doors immediately aft of the intake and no engine anti-icing bleed air heating is available. The resulting surface temperatures measured in this region exceed +15°C even in the most severe icing conditions in high-speed cruise. While adequate to prevent direct impingement ice, this is insufficient to evaporate all liquid water running downstream from the stagnation line given the available heated extent.

To further reduce the amount of runback ice accretion on the upper side of the engine intake, where ingestion of shed ice by the engine in low-speed or hovering flight may occur, KAI conceived the *edgehill* concept shown in Figure 3. Flight and wind tunnel testing has demonstrated that the edgehill helps to reduce runback ice accretion in a number of ways:

- *Negative mass flux due to water stripping*
  Runback water that is aerodynamically forced over the tip of the edgehill was found to strip away from the surface as the fluid inertia forces exceed the surface tension. The result is a light frost on the downstream side of the edgehill without the concentrated ice accretion typical of runback ice.

- *Increased evaporation*
  Runback water that is forced to travel in a lateral direction parallel to the edgehill more readily evaporates due to the extended path traveled over a heated surface. In conditions with high water catch rates, residual runback ice accretes at the corners of the edgehill in a region of less concern for engine ice ingestion.

- *Increased ice shedding frequency*
  In relatively cold icing conditions, direct impingement ice may accrete on the tip of the edgehill. However, due to the small contact area and prevailing aerodynamic environment, accreted ice has been demonstrated to shed both frequently and consistently, thereby preventing large-scale ice accretions.

The protected area of each intake is divided into three electrically-insulated heater mats connected by a temperature controller supplying three-phase power. The temperature controller aims to achieve the highest possible surface temperature while preventing cowling material overheat in the high power density regions of the heater mat. The controller logic provides redundancy by acquiring multiple interlaminate temperature sensors.

Despite tight tolerances on heater mat gap width, the location and orientation of the gaps between heater mats needs to be carefully considered to avoid cold lines in areas of high collection efficiency and comparatively low power density. In case such cold lines cannot be avoided, it is preferred to orient the heater mat gaps in streamwise direction such that potential ice accretion forms a natural shadow region further downstream. This is the approach that was taken at the upper side of the KUH-1 engine intake. Figure 4 shows an example of the residual ice accretion that forms on the heater gap below the stagnation line where power density is lowest.

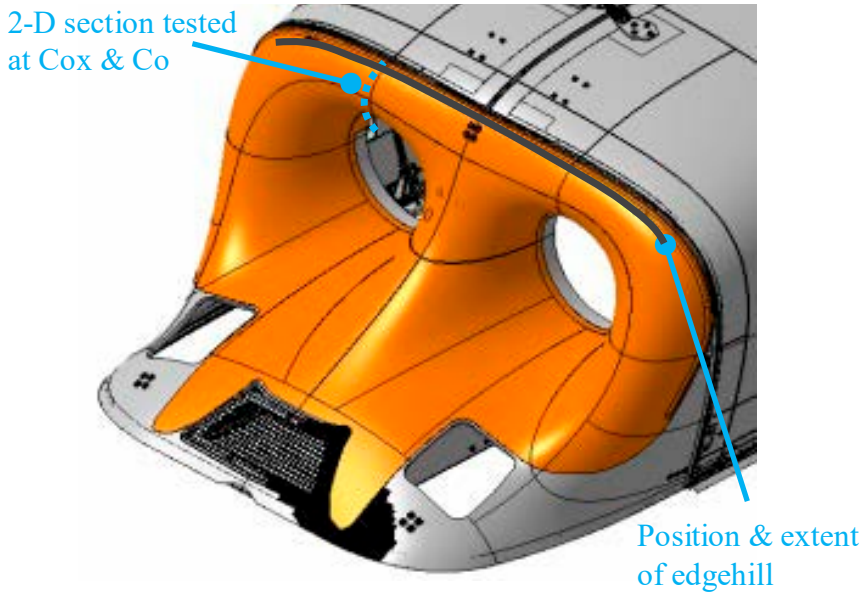

Figure 2: CAD rendering of KUH-1 engine air intake cowling showing extent of electrothermal heater mat and edgehill.

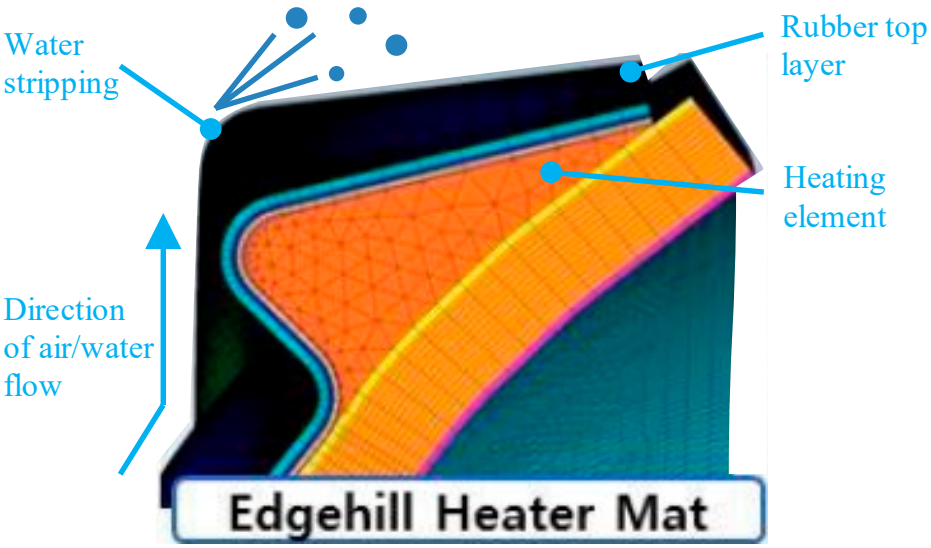

Figure 3: KAI edgehill heater mat concept. The layup shows the cowling structure at the bottom and the resistor element wrapped around filler material to form the hill.

2.2 Test activities

The KUH-1 engine intake ice protection system has been subjected to two separate full-scale icing wind tunnel tests; one at CIRA in Italy, and one at RTA in Austria. The related test activities are described in [3, 4]. In an intermediate effort, full-scale 2-D icing tests were conducted in the 0.7 x 1.2 m test section of the Cox & Co Icing Wind Tunnel (IWT) to verify the effectiveness of the edgehill concept described in the previous paragraph. The model for this test consisted of a 2-D airfoil-shaped section, the leading edge of which is representative of the centreline cross-section of the KUH-1 engine intake highlight, see Figure 2. During the test, multiple heater mat and edgehill configurations were investigated, each interchangeably installed on the same rigid substructure. Figure 5 shows one of the model configurations horizontally mounted inside the IWT test section. To achieve a representative heat transfer, the layup of the composite leading edge is identical to that of the KUH-1 engine intake cowling. A still-air convective boundary condition exists internally, neglecting potential engine heat sources. Temperature instrumentation consisted of both interlaminate RTDs and surface thermocouples. The thermocouple wire was imbedded inside the upper rubber layer of the heater mat to minimize the disturbance to the boundary layer and the surface water film. The associated gaps in the heater mat were filled with an epoxy with thermal conductivity similar to that of rubber.

The drop impingement and collection efficiency of the 3-D geometry in reference flight conditions were matched in the IWT by setting the angle of attack of the test article to reproduce the correct stagnation line position and scaling the Median Volume Diameter (MVD) of the icing spray according to the modified inertia parameter *K0* [5]. The IWT test conditions were defined based on a comparison between 2-D LEWICE calculations and 3-D full airframe CFD results obtained by AeroTex UK, assuming nominal engine mass flow rates calculated by KAI. An example result for collection efficiency can be found in Figure 6 which shows a satisfactory match in predicted drop impingement, particularly between the stagnation line and the edgehill, which is the primary region of interest for matching the upper surface runback ice. The stagnation line position was verified at the start of testing by monitoring the movement of the water film at the leading edge at above-freezing test conditions. The predicted boundary layer heat transfer coefficient, which is a dominant factor in the convective heat loss, was also evaluated numerically, but a direct code-to-code comparison was not possible due to differences in assumed average surface roughness (a parameter that is not tunable in the commercial version of LEWICE).

The effect of the edgehill is visible in Figure 5 as a large area of white frost on the upper downstream surface. The frost is formed as runback water is stripped from the tip of the edgehill and is partially re-entrained, impacting with the surface in a randomly distributed pattern. By contrast, on the left-hand side of the edgehill looking downstream (where the protected extent is larger than is possible on the KUH-1 engine intake cowling) the runback water is observed to form a ridge immediately aft of the heated area. While the aerodynamic impact of such ice formations is not a primary concern for the engine intake, the possibility of shed ice ingestion is.

The test result shown in Figure 5 was obtained in test conditions scaled to achieve Weber number similitude. The Weber number is a dominant factor in the formation of runback ice in general [6], and even more so for a geometry including edgehill. At colder test conditions where positive surface temperatures could not be achieved without exceeding material temperature limits, Reynolds number scaling was applied to match the free-flight convective heat loss. The resultant ice accretions were observed to increase due to the fact that the reduced aerodynamic forces limited the shedding frequency.

The 2-D test activities enabled the identification of the most effective edgehill geometry, as well as the associated requirements for electrothermal power density. The KUH-1 engine intake design was subsequently modified in preparation for qualification testing in the RTA IWT.

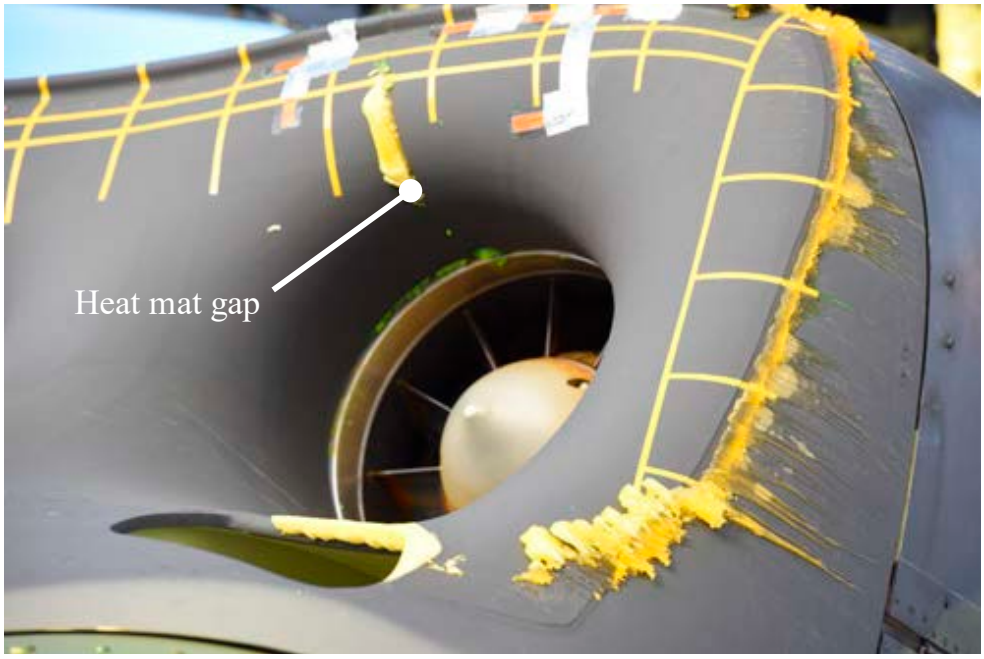

Figure 4: 2017/2018 artificial icing flight test results showing impingement ice (dyed yellow) on cold line between heater mats above the engine and runback ice aft of the lateral limits of the heated area.

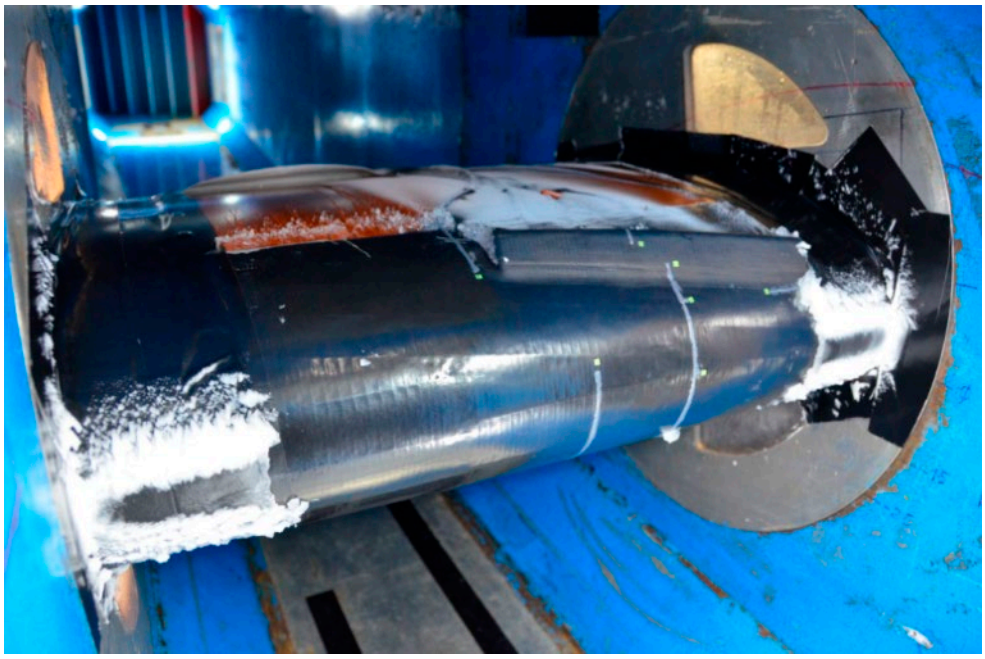

Figure 5: 2-D model of engine intake highlight with partial-span sloped edgehill installed inside Cox & Co IWT test section. The outboard 10 cm on each side is unheated.

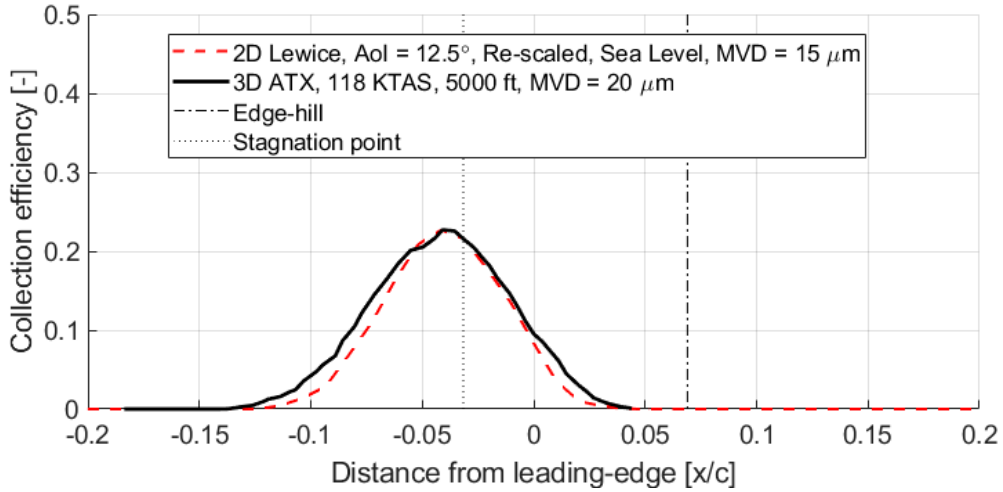

Figure 6: Predicted match in collection efficiency between 3-D full airframe level flight CFD and 2-D LEWICE calculation of IWT model in scaled test conditions and without wall-effects.

3 Wire cutter anti-icing

3.1 Design description

The upper wire cutter of the KUH-1 wire strike protection system is located in close proximity to the engine air intake. To manage the risk of engine damage due to ice ingestion, the wire cutter is anti-iced to prevent the formation of ice accretions above the engine ice ingestion limit determined by the engine manufacturer.

The metal structure of the KUH-1 wire cutter is characterized by high conductive and convective heat losses, particularly through the side surfaces of the deflector, see Figure 7. Moreover, due to the stringent structural strength requirements, large parts of the cutter are solid, making it difficult to incorporate provisions for heating. The sharp features of the cutter and the deflector leading edge further complicate the distribution of heat towards the leading edge where drop impingement rates are highest. To cope with these design challenges, the KUH-1 wire cutter anti-icing system incorporates both electrothermal heater coils and engine bleed air, as shown in Figure 7.

The key to the success of this type of a design lies in concentrating the heat as far forward towards the leading edge as possible. At the deflector, this is achieved by using imbedded temperature-controlled coil heaters. The cutter area also feature a coil heater, but requires additional anti-icing by means of engine bleed air, because the geometry and structural requirements do not allow for the integration of an internal heat source close to the leading edge. Alternatives using, e.g., heatable coatings, were considered, but ultimately not pursued in favor of reliable and proven technologies that, moreover, did not impact the qualification for wire strike protection.

The coil heaters are arranged in Y-configuration with two temperature controllers supplying three-phase electrical power. In the event of a single controller failure, the complete structure remains anti-iced with a 50% reduction in electrothermal power and full engine bleed air. The layout of the deflector coil heater is designed such that the surface temperature is highest at the midpoint of the deflector. Ice accreted in degraded conditions is effectively cut in half, thereby reducing the maximum shed ice size by a factor of two.

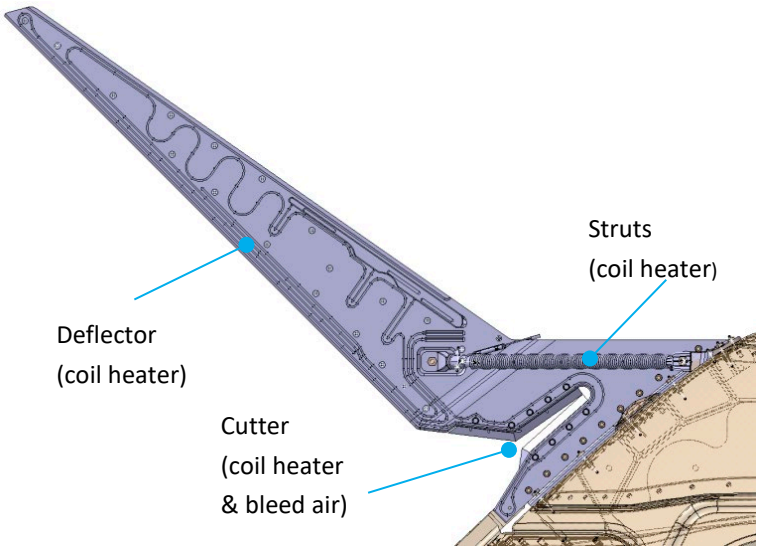

Figure 7: KUH-1 wire cutter with distributed means of anti-icing.

3.2 Test activities

Initial icing flight testing conducted in 2015/2016 [1] revealed inadequate anti-icing of the upper wire cutter deflector at the cold end of the KUH-1 qualification icing envelope. The shortcoming was addressed by a redesign of the internal coil heater layout and an increase in electrical power. To confirm that the modified design performed satisfactorily prior to the second and final icing flight test campaign, an intermediate component-level icing test was performed in the Cox & Co IWT. The test set-up is shown in Figure 8.

The wire cutter was mounted on an approximately flat fairing plate, the angle of which could be adjusted between 0° and 17° nose-down. The fairing plate was partially deiced by intermittently supplying a variable voltage to a heater foil bonded to the leading edge of the fairing. The test set-up provided relatively well-defined flow conditions suitable for post-test code correlation, and a basic level of control to more accurately replicate the environment of the wire cutter installed on the aircraft. Prior to testing, 3-D CFD and drop trajectory analyses were performed to quantify the installation effects on the aircraft. For example, the data plotted in Figure 9 depicts the local velocity deficit and drop trajectories in a 2-D plane through the wire cutter. The velocity profile and Liquid Water Content (LWC) depletion directly upstream of the wire cutter were extracted and used to define correction factors for the 2-D test. In consideration of the change in flow and impingement angles along the length of the wire cutter, the angle of incidence for the 2-D test was adjusted according to the area of interest. Similar to the 2-D engine intake test, altitude scaling was applied by matching stagnation point recovery temperature, stagnation water catch rate, modified drop inertia parameter, and either Reynolds number or Weber number.

The 2-D wire cutter IWT test successfully demonstrated adequate anti-icing of the deflector. Close-up inspection of the test article revealed a complex ice accretion pattern near the unheated cutter that was exacerbated by protruding bolts and nuts located aft of the leading edge, particularly in glaze ice conditions. An example can be found Figure 10, which shows the ice accreted near the start and end of a 30-minute Continuous Maximum Icing (CMI) test point. Following the IWT test, the design was further optimized by fairing in the bolt heads where possible, extending the internal coil heater, and ultimately providing additional anti-icing for the cutter by means of engine bleed air. The modified wire cutter design was verified in a second IWT entry, and finally through the icing flight test activities. The final configuration as flight tested is shown in Figure 11.

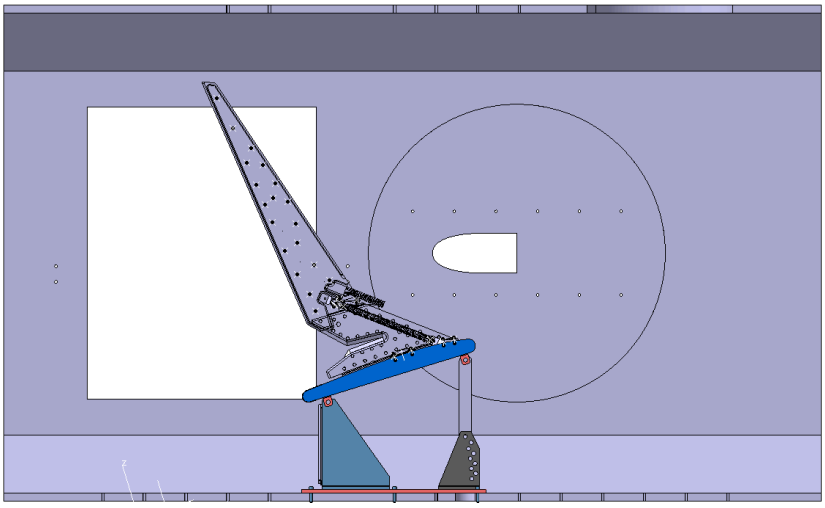

Figure 8: Side view of wire cutter test set-up in Cox & Co 0.7 x 1.2 m IWT test section (wind from the left). The angle of incidence is adjustable at fixed increments between 0° and 17° nose-down.

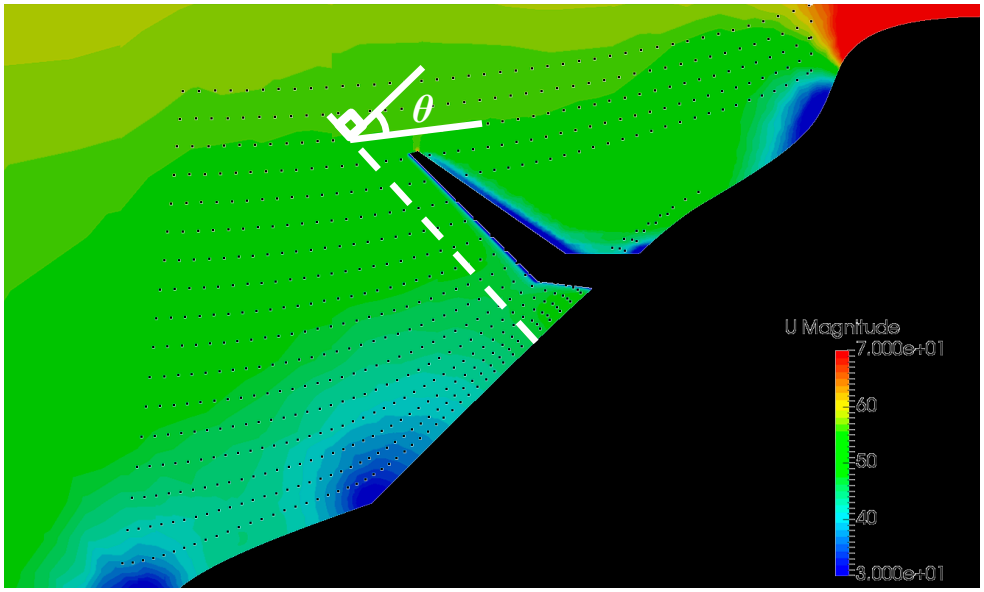

Figure 9: 2-D splice of 3-D CFD and drop trajectory calculations aimed at quantifying the installation effects surrounding the upper wire cutter on the KUH-1. The colour contours correspond to the velocity magnitude. The dotted lines represent computed drop trajectories.

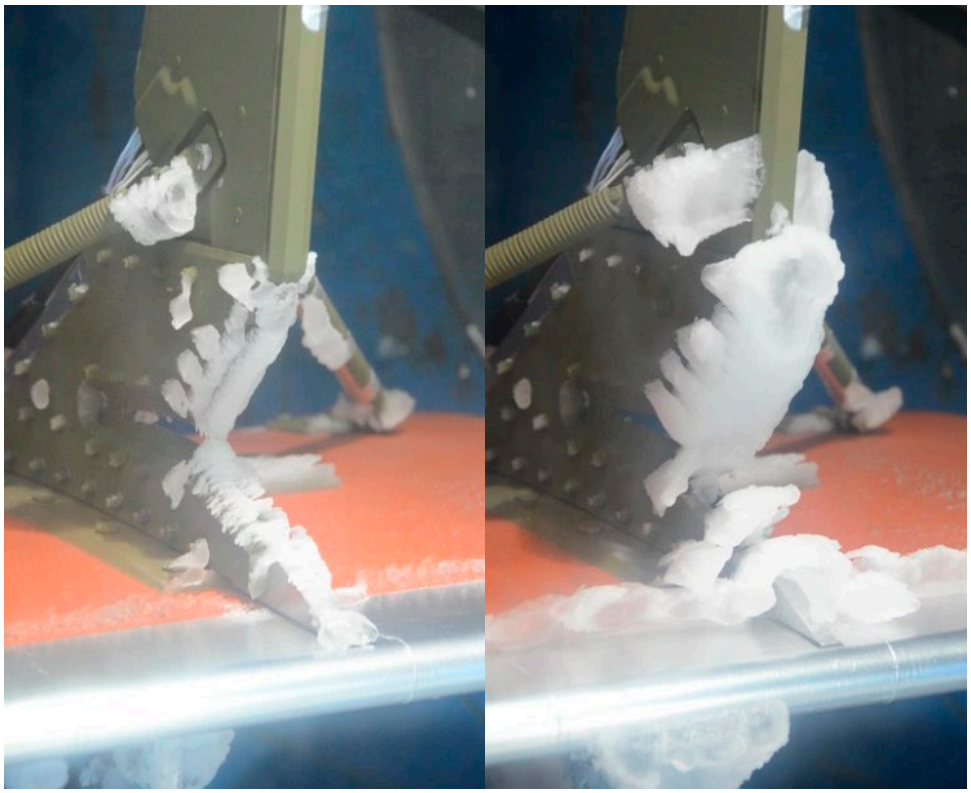

Figure 10: Ice accretion on unheated scissor at -10°C after 5-min (left) and 30-min (right) CMI exposure at high-speed cruise conditions.

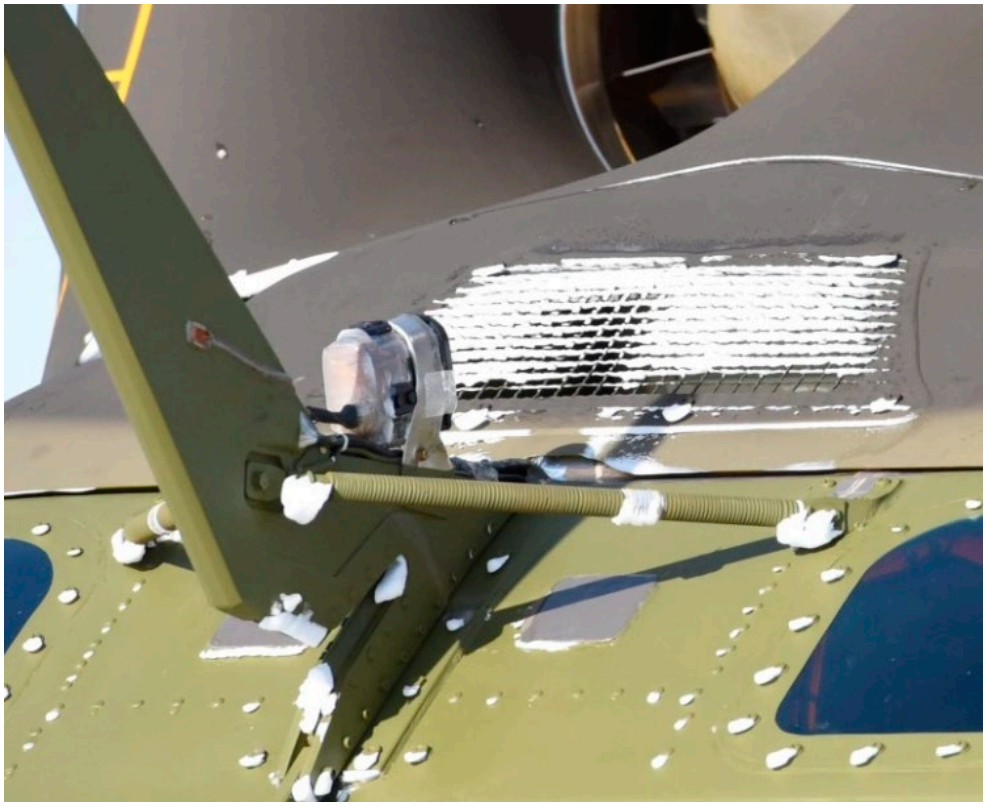

Figure 11: Final configuration of KUH-1 upper wire cutter as tested in 2017/2018 icing flight test campaign. Photo taken in-ground after natural icing exposure.

4 Rotor ice protection system

4.1 Design description

The KUH-1 Main Rotor Ice Protection System (RIPS) started out as a legacy design. The main rotor is deiced by five heating zones distributed in a chordwise direction along the leading edge of the blades as shown in Figure 12. To maintain symmetry while limiting the electrical power requirements, the four-bladed rotor is deiced two opposing blades at a time. The deicing logic is governed by the Outside Air Temperature (OAT) and the Liquid Water Content (LWC). The LWC measurement is provided by a Rosemount/UTAS ice detector located near the nose of the aircraft. An Ice Rate Meter Panel (IRMP) in the cockpit provides real-time feedback of the measured LWC to the pilot. If the flight crew has a concern regarding the accuracy of the indicated LWC, a manual mode of operation is available providing discrete control over the heater off-time.

In the legacy design, the heater on-time was fixed at one of two values, with a hard switch at a given OAT. This design maintained a clean leading edge, but at the expense of runback ice accretions over a large part of the icing envelope. The associated torque rise was stabilized, but did not display the limit-cycle characteristic expected of an optimized deicing system. Following the first icing flight test campaign, the heating sequence, as well as the heater on-time (ONT) and off-time (OFFT) equations, were modified to reduce or eliminate runback ice accretion. Figure 12 provides an overview of the new logic adopted for the ONT and OFFT [7]. To account for in-flight variations in icing intensity, the RIPS controller continuously compares the elapsed OFFT with the OFFT computed based on a running average LWC.

The ONT is expressed as a linear function of the OAT and reflects the time required to increase the blade surface temperature from the local recovery temperature at a given radial station to a marginally positive value adequate for deicing. The OFFT is inversely proportional to LWC and is intended to provide a constant inter-cycle ice thickness independent of icing intensity. The ONT is not a function of LWC since the blade surface, by design, is insulated by the ice accreted during the heating OFFT and evaporative losses do not play a significant role on the surface heat balance during the ONT. Assisted by centrifugal forces and vibratory loads, surface temperatures at or even slightly below the freezing level are sufficient to deice helicopter rotor blades [8]. Moreover, it is undesirable to operate at substantially higher surface temperatures as this increases the risk of runback ice accreting aft of the protected area. Margin is required, however, to account for, e.g., degraded electrical power generation, chordwise variations in the markedly transient heater temperature, measurement error, etc.

In the case of the KUH-1, the constants of the linear ONT law shown in Figure 12 have been derived using an empirical model of rotor blade surface temperature, initially tuned against flight test data obtained during the 2015/2016 icing flight test campaign [2]. The constants C_1 and C_2 were selected to achieve peak surface temperatures at the chordwise centre of each heating zone equal to at least 0°C across the whole blade span at outside air temperatures within the design envelope. A minimum ONT of 2 seconds is employed at OATs warmer than -5°C to provide sufficient time to overcome the thermal inertia of the blade and affect a positive response at the surface. That being said, the positive effects of supplying additional heat at these relatively warm outside air temperatures is limited by the small radial extent of ice accretion and the risk of generating more runback ice.

The constant C_3 that controls the OFFT has been defined based on a target inter-cycle stagnation point ice thickness Δ_R that is considered acceptable in terms of peak torque rise and impact risk associated with shed ice, and is large

enough to promote shedding under centrifugal and aerodynamic loads with minimal melt/runback water. If the ONT is set to achieve marginally positive peak surface temperatures, the time for the blade surface to cool down below freezing will be negligible in all but the cases where the recovery temperature is close to freezing. Knowing the stagnation ice thickness at a given rotor blade section is governed by the average velocity equal to the speed of rotation, the OFFT constant can then be simply calculated by:

$$C_3 = \frac{\rho_{ice}\Delta_R}{R\Omega\beta_0} \quad (1)$$

The ice density ρ_{ice} and stagnation collection efficiency β_0 depend on the icing condition and airfoil geometry, but the parameters in equation (1) generally will not vary much between aircraft.

The remaining variable is the heating sequence, i.e., the order in which the individual spanwise zones are heated. The aim here is to deice the leading edge as soon as possible as this is the primary source of drag [7, 8]. The remaining zones may have some measure of direct impingement, but are mainly there to accrete and subsequently shed runback ice generated by the leading edge zones. Following the 2015/2016 test campaign, the KUH-1 main rotor IPS heating sequence has been redefined as 1-3-2-4-5 in order to provide time for Zone 1 to cool down below freezing before heating Zone 2 on the upper surface.

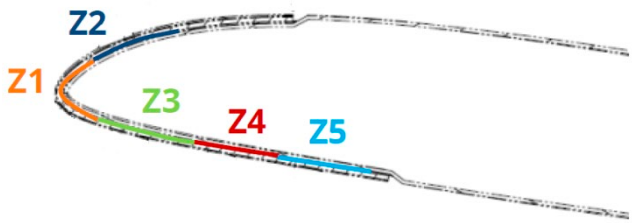

-30°C ≤ OAT ≤ -5°C		-5°C ≤ OAT ≤ 4°C	
ONT [sec]	OFFT [sec]	ONT [sec]	OFFT [sec]
OAT x C_2 + C_1	C_3/LWC	2	C_3/LWC

Figure 12: Chordwise distribution and numbering of KUH-1 main rotor blade IPS heating zones and AUTO mode heating logic (same for all heating zones).

4.2 Test activities

Due to time constraints in the KUH-1 IPS development and qualification schedule, no IWT test activities were performed on the main rotor IPS. The performance with the modified logic was demonstrated directly through artificial and natural icing flight testing. The primary aim of the RIPS flight test activities was to demonstrate an improved and periodic icing torque rise evident of reliable and complete main rotor deicing. Initial testing focused on artificial icing with the Helicopter Icing Spray System (HISS) tanker in CMI conditions near the previously established critical OAT of -15°C. However, given the confidence in the safe operation of the system garnered through the first flight test campaign in 2015/2016, natural icing test flights were performed whenever the icing forecast was promising. In light of the empirical nature of the tools used to define the new RIPS heating logic, arrangements were made with Cox & Co, the supplier of the digital control unit, to enable rapid turnaround for software changes pending full verification and validation at a later stage.

HISS testing of the main rotor IPS primarily consisted of 30-minute CMI rotor immersions at 120 KIAS. A data loader was used to set the LWC for RIPS operation based on the HISS spray calibration. Stable level flight data records were taken of the engine torque before and immediately after immersion to remove the effects of collective movement

required for station keeping and the HISS wake downwash and turbulence. However, the torque rise often deteriorated quickly after exiting the icing spray due to (RIPS OFF) ice shedding, invalidating the post-icing torque record. Therefore, estimates of icing torque rise during rotor immersion were also made by applying an approximately constant torque rise correction for the HISS effect. Ultimately, the comparison with data obtained in natural icing conditions revealed a tendency for somewhat higher icing torque rise in natural conditions.

To verify the proper operation of the RIPS and demonstrate acceptable spar temperatures, KAI instrumented the main rotor blades with spar and erosion shield surface temperature sensors. To synthesize the large amount of data recorded, Figure 13 presents the minimum and peak blade surface temperatures measured at 26% radius across all natural icing flights, averaged over OAT bins that are 2.5°C wide. The data exemplifies the trending that is desired of a deicing system, i.e., minima sufficiently cold to accrete ice, and maxima adequate for deicing yet not conducive to runback ice accretion. Note that the minimum temperature occurs at the end of the OFFT with the iced surface close to the local recovery temperature.

To explore the effect that on-board LWC measurement accuracy may have on the icing torque rise in natural icing conditions, a dedicated HISS flight was performed near the critical OAT with the data loader LWC set 30% above and below the calibrated value. No substantial differences in torque rise or vibration characteristics were observed. While this result does not explain the discrepancy between the HISS and natural icing torque rise, it does provide confidence in the operation of the RIPS in the presence of realistic LWC measurement inaccuracies.

In addition to analysing level flight engine torque, measurements of the 2/rev vibrations in the fixed frame provide a reliable, albeit qualitative, metric for the RIPS effectiveness. Figure 14 shows an example time trace of the 2/rev vertical cabin vibrations during an extended flight in natural icing conditions. In between RIPS heating cycles, ice accretes on all four blades in an approximately symmetric fashion such that the 2/rev vibration level is approximately equal to that of the clean rotor. Deicing of the leading edge zones of the first blade pair is accompanied by a measurable increase in 2/rev vibration magnitude. Following the deicing of the second blade pair, the vibrations return to their nominal values. The change in 2/rev vibration over time, therefore, provides evidence of effective and symmetric main rotor deicing. If cyclic changes in 2/rev vibration are not accompanied by distinct changes in torque rise, this is an indication that residual ice remains on the rotor blades (e.g., runback ice).

Figure 15 provides an overview of the normalized increase in 2/rev vibrations during main rotor deicing throughout the tested OAT envelope. The trend highlights -15°C as the approximate critical icing temperature for the main rotor. At warmer conditions the reduction in radial icing extent reduces the mass imbalance during deicing. At the cold end of the icing envelope the mass of accreted ice is constrained by the effects of sublimation and erosion over the comparatively long OFFT.

The flight test activities demonstrated a robust control of icing torque rise with no notable change in handling qualities. The modified main rotor IPS heating logic enabled a substantial reduction in icing torque rise sufficient to meet the ROKA customer performance requirements.

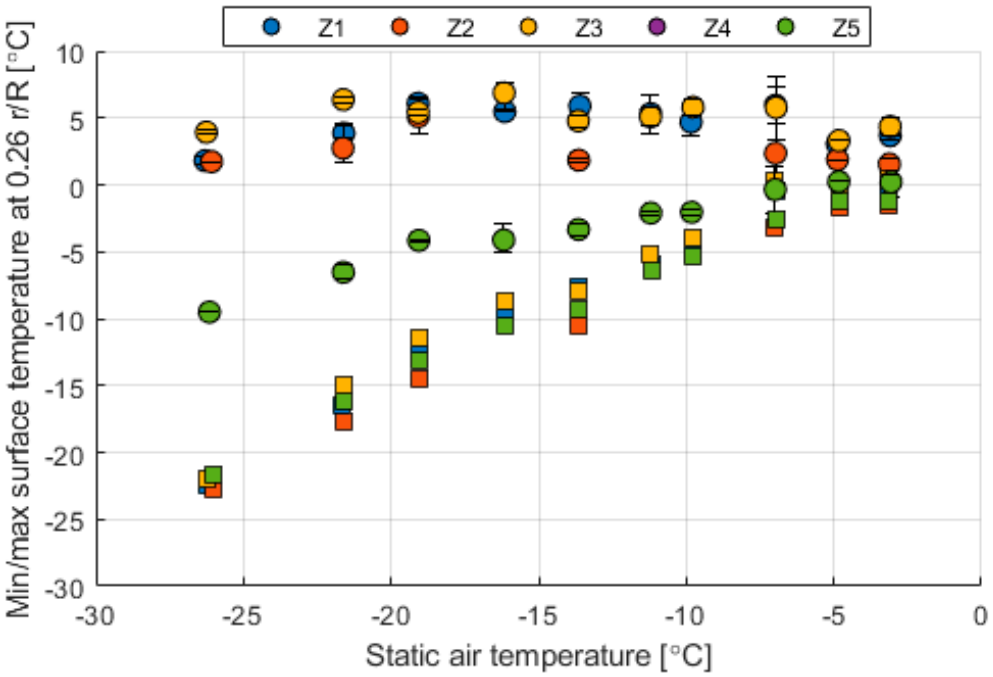

Figure 13: Measured in-icing minimum (square) and maximum (circle) main rotor blade mid-zone surface temperatures averaged over OAT bins that are 2.5°C wire. Each data point represents the average temperature over all natural icing flights in a given bin.

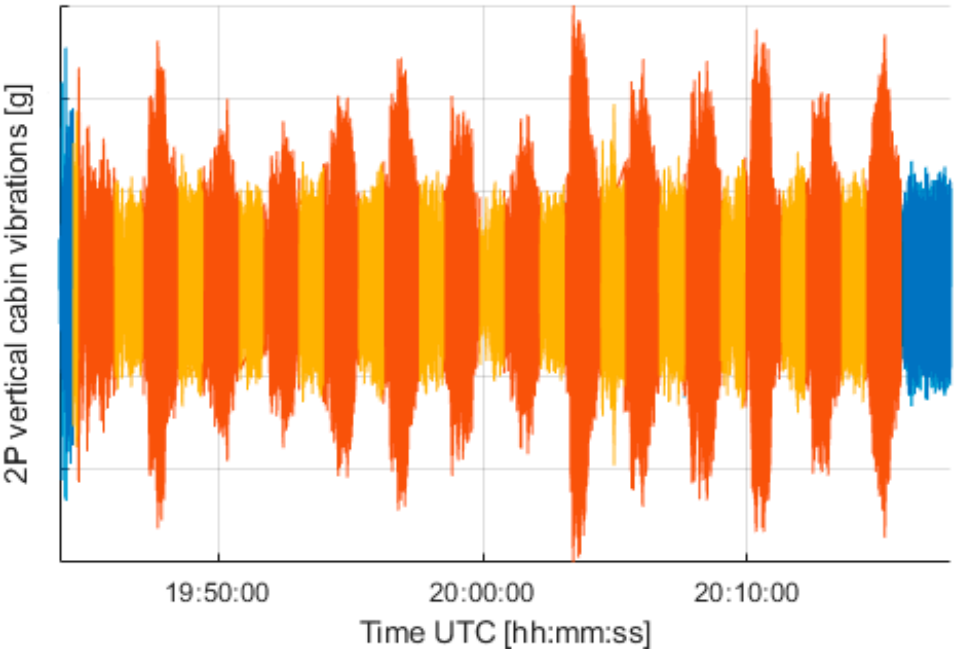

Figure 14: RIPS deicing evident in limit-cycle variations in time-trace of 2/rev (2P) vertical cabin vibrations. The red sections of the trace indicate the main rotor HEAT ON period of both blade sets, whereas the yellow sections correspond to the IDLE time in between heating cycles.

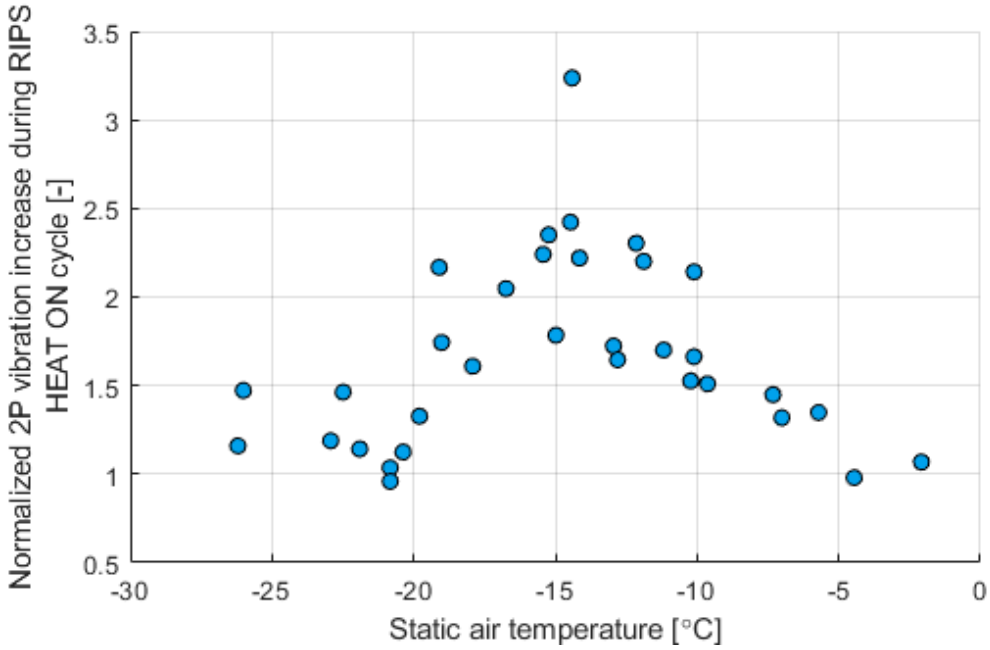

Figure 15: OAT effect on RIPS deicing performance as evident in variations in 2/rev (2P) vertical cabin vibrations. The data is normalized by the in-icing vibration level recorded during the RIPS HEAT OFF time.

5 Icing flight testing

The KUH-1 icing qualification program included two icing flight test campaigns. In both instances, the artificial icing flights were performed with the HISS tanker operated by the US Army out of Marquette, MI [1]. Natural icing flight testing was conducted across the Upper Peninsula and to the east of Lake Michigan, both in the state of Michigan. The KUH-1 test aircraft was equipped with high-definition cameras for self-documentation and a Droplet Measurement Technologies Cloud Combination Probe (CCP) for cloud characterization. The CCP was regularly compared to the optical probes of the US Army C-12 chase plane during HISS cloud calibration. Remote icing forecasting and in-flight guidance was provided by FlightCast LLC in combination with in-situ support from the C-12. Forecasts included information on icing probability, optimum icing altitude in the target area, estimated OAT, LWC and MVD, potential Supercooled Large Drop (SLD) threats, etc. When available, the C-12 confirmed the forecast conditions and proposed the airspace section and block altitude within which the icing conditions were optimal, before exiting the clouds in coordination with Air Traffic Control.

The majority of the testing took place within the Uniform Daylight Period. In accordance with the anticipated guidance in AC 29-2C, however, a single dedicated night icing flight was conducted to demonstrate suitable icing cueing during night time operations to be used in case of an unannunciated failure of the non-redundant Ice Detection System (IDS). The selected cueing, visual or otherwise, must be noticeable to the flight crew prior to unsafe ice accretions accumulating on the airframe or rotor blades. All cockpit and external lights remained extinguished until the test was concluded and use of a handheld flashlight was restricted because of the associated additional crew workload. The flight crew was briefed on the geographical location where icing was expected, but not the exact conditions. It was found that the ambient light from the cockpit is not sufficient for visual icing cueing at night. Rather than a visual cue, the pilots reported strong icing cues in the form of increased torque rise, followed soon thereafter by increased vibrations. Based on the data recorded by the CCP, the detection time is estimated at 2 minutes in CMI conditions, independent of airspeed.

In post-processing, the natural icing encounters were analysed and categorized according to icing condition and flight parameters. The DEF STAN 00-970 (design) icing envelope selected for the KUH-1 qualification basis does not include LWC variations with MVD and does not define an LWC scale factor for horizontal cloud extent. A distance-based representation as typically accepted for civil icing certification [9] was, therefore, not possible. Instead, the Korean military airworthiness authorities took the position that qualification test data was to be acquired over single-cloud icing encounters at least 30-minute in duration at an airspeed of approximately 120 KIAS, defined as the never-exceed speed (VNE) in icing for the KUH-1. To not further constrain the data gathering, no specific requirement was set for MVD other than the need for a stable encounter. Figure 16 provides an overview of the tested envelope of the 2017/2018 test campaign in comparison with the DEF STAN envelopes.

Most of the natural icing encounters inside the tested envelope fell short of the 20 µm MVD DEF STAN envelope (which was found to be exceedingly rare, even in the clean air of the UP). This shortcoming was deemed acceptable in part because the engine air intake, the primary system affected by drop size owing to its blunt geometry, was previously qualified through IWT testing, and additional evaluation through natural icing flight testing is not required according to AC 29-2C.1093. Moreover, it was recognized that the HISS test activities provided conservative test conditions with MVD typically exceeding 20 µm. In fact, the water catch rate of the engine air intake, computed taking into account the effect of MVD on stagnation collection efficiency β_0, was close to DEF STAN PMI levels for all of the high-LWC CMI HISS test points.

The CCP was the primary instrument used for cloud characterization. Despite the fact that the CCP is not widely considered as a reference instrument for LWC, it provided the only available reference for verifying the installed accuracy of the Rosemount IDS. An installed accuracy of ±30% with respect to the CCP LWC was required by the airworthiness authority. This tolerance applied both to the LWC data sent to the RIPS controller and the LWC indication in the cockpit on the IRMP. Following positive experience with camera-based instrumentation in previous flight test activities [10], a similar set-up was proposed to measure the LWC indicated by the IRMP. Figure 17 shows an example comparison between the analog signal provided to the RIPS controller and the data digitized from video recordings of the IRMP. The ±10% error band was considered adequate demonstration that the IRMP and input to the RIPS controller were in agreement.

In addition to the basic data gathering flights, numerous artificial and natural icing flights were aimed at demonstrating acceptable power-off autorotation characteristics with maximum inter-cycle ice on the rotor blades as required by AC 29-2C.1419. For safety reasons the power-off landing itself is not demonstrated through flight testing. Instead, the test objective is to demonstrate the ability to enter and maintain a steady autorotation after icing within acceptable rotor speed (NR) limits. In particular, it is the lower limit of rotor speed that is of concern since the additional drag of the rotor ice accretions will reduce the power-off rotor speed, potentially below the limit beyond which the gearbox-driven electrical generators can power the RIPS and other vital electronics. The autorotation demonstrations were conducted RIPS OFF and were initiated as closely after exiting icing as altitude minima allowed. Note that in a real emergency requiring autorotation, the RIPS would remain operative and manual mode operation would enable the pilot to force an immediate deicing cycle (time permitting). Figure 18 presents KAI's synthesis of the predicted loss in power-off rotor speed at best-climb speed (VY) due to ice accretion. The iced rotor trend is based on the empirically verified relation between loss in power-off rotor speed and icing torque rice. It can be observed that, in all conditions, positive margin is available with respect to the steady power-off minimum rotor speed, thus assuring safe autorotation characteristics.

The 2017/2018 KUH-1 icing flight test campaign included 31 artificial icing sorties, among which were several repeats to demonstrate repeatability. In addition, 25 productive sorties were flown in natural icing conditions at static air temperatures between -4.5°C and -26.3°C. On most flights, observers of the ROKA and/or Korean airworthiness authorities were on-board the test aircraft to witness the testing. The test experience and data gathered were sufficient to successfully conclude the KUH-1 icing qualification in July 2018.

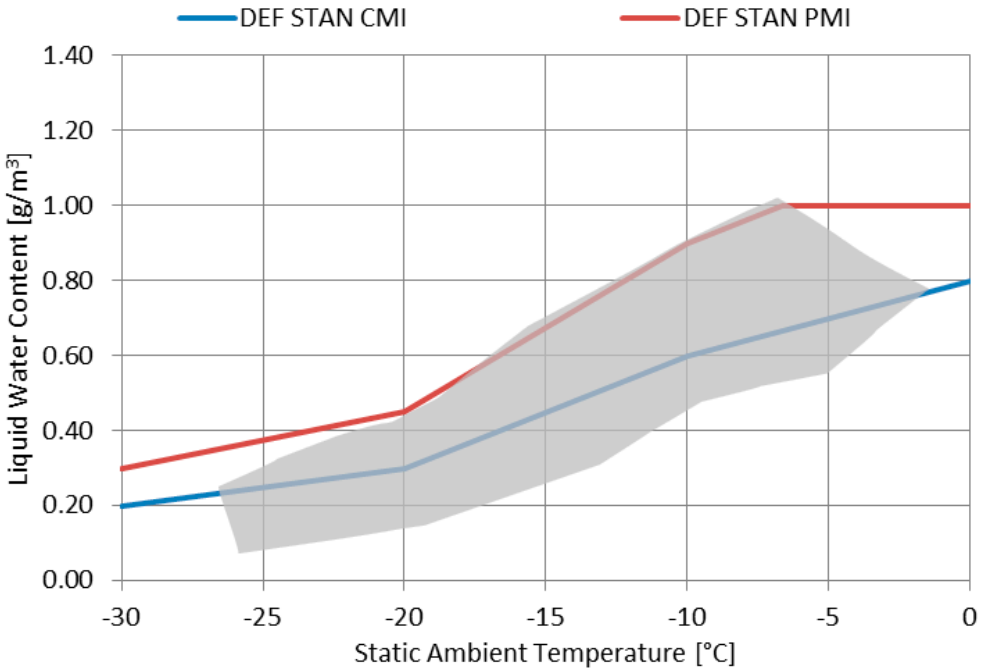

Figure 16: Tested envelope of KUH-1 artificial and natural icing test points achieved in the 2017/2018 test campaign. The natural icing data points included in the envelope have been obtained at average airspeeds close to 120 KTAS.

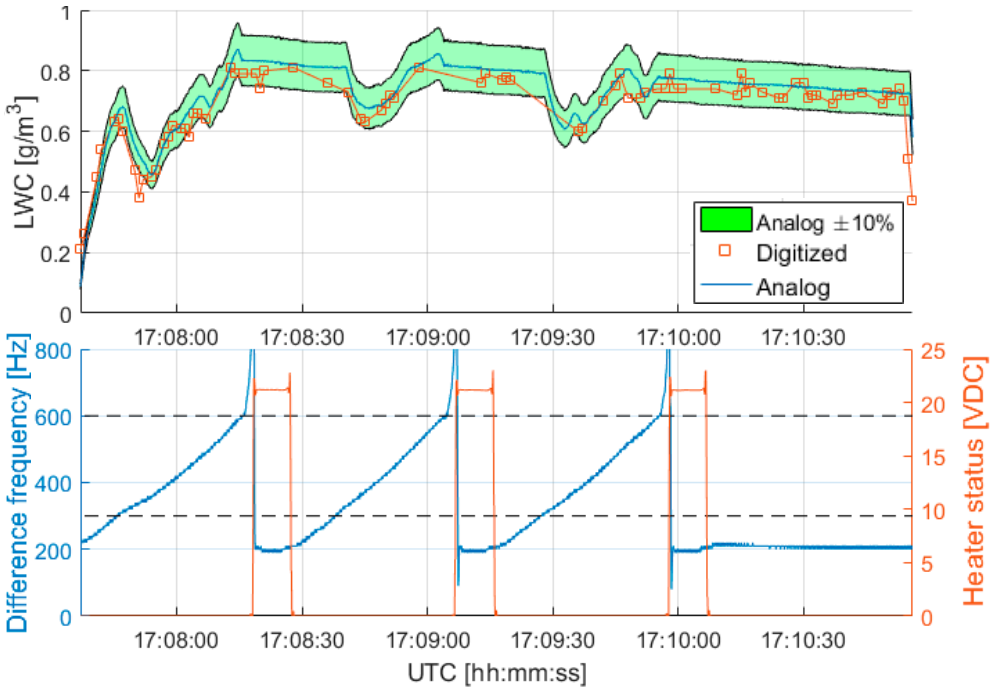

Figure 17: Comparison of analog LWC at RIPS controller input and LWC digitized from video recordings of IRMP. The IDS provides a real-time LWC measurement when the difference frequency of the Rosemount probe is between the bounds indicated by the dashed black lines.

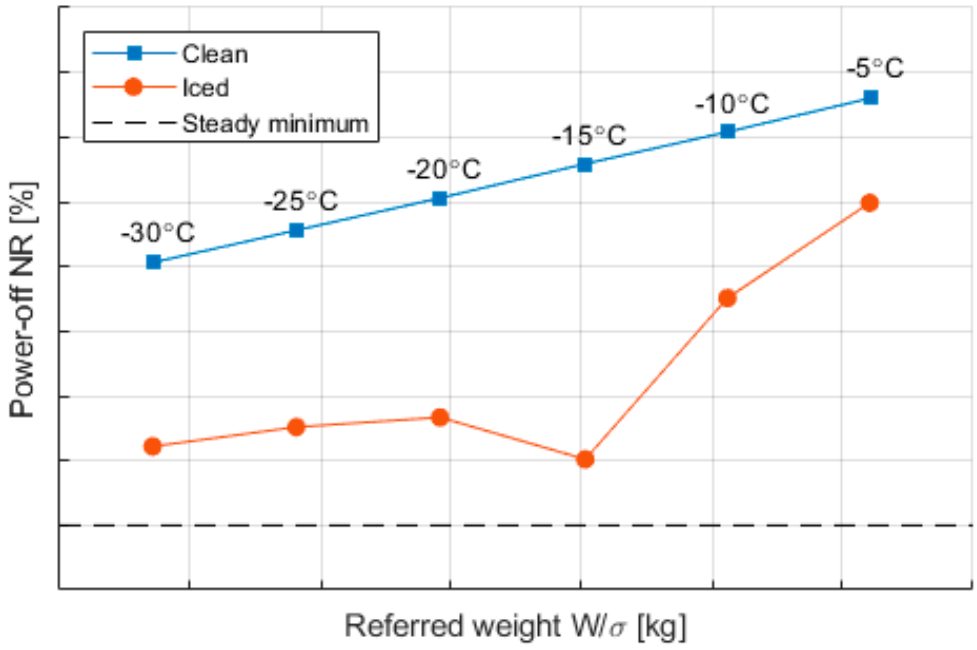

Figure 18: Reduction in power-off autorotation rotor speed at VY due to maximum main rotor inter-cycle ice accretion. The KAI analysis takes into account the effect of OAT on minimum referred weight with minimum crew and reserve fuel. The iced rotor trend is based on an empirically verified relation between loss in power-off rotor speed and icing torque rice.

6 Conclusions

Under the pressure of an ambitious delivery schedule, the KUH-1 icing qualification program has seen a large number of test activities over a relatively short period of roughly three years. The first icing flight test campaign was performed in 2015/2016 and included both artificial icing testing with the US Army HISS tanker, as well as flight testing in natural icing conditions. The flight test activities were followed by numerous icing wind tunnel tests aimed at further optimizing the KUH-1 IPS prior to the final flight test campaign in 2017/2018.

Following the first flight test campaign, the KUH-1 engine intake IPS production design was modified to achieve a larger protected area with optimized power density distribution and unchanged power budget. A novel edgehill concept was introduced that enabled a substantial reduction in runback ice accretion in a region where the heated area could not be extended. The subsequent ground and flight test activities have demonstrated satisfactory intake anti-icing capability throughout the qualification icing envelope with no safety-critical ice accretions.

The upper wire cutter of the KUH-1 is anti-iced by a combination of electrothermal coil heaters and engine bleed air in order to prevent engine ice ingestion. Multiple design iterations were tested at component-level in the Cox & Co icing wind tunnel. This testing was instrumental to verifying the anti-icing performance prior to final qualification flight testing in 2017/2018.

The main rotor IPS was qualified directly through artificial and natural icing flight testing with no prior or intermediate icing wind tunnel testing. The heating logic was tuned using an empirical model of rotor blade surface temperature derived using data gathered during the first flight test campaign. The modifications to the main rotor IPS heating logic enabled a substantial reduction in icing torque rise, sufficient to meet the ROKA customer performance requirements, together with consistent deicing and acceptable vibration characteristics.

The icing flight test activities further demonstrated a useable visual cue for the presence of icing condition at night, acceptable accuracy of the installed IDS LWC measurement and cockpit indication, as well as safe power-off autorotation characteristics. The US Army HISS tanker provided conservative high-MVD test conditions extending over a large part of the certification icing envelope. The coldest qualification test points were obtained in natural icing conditions over the state of Michigan, reaching temperatures as low as -26.3°C.

Despite the aggressive development schedule, the hard work and collaboration of all parties involved has led to a successful conclusion to the KUH-1 icing qualification in July of 2018.

7 References

1. Van 't Hoff, S.C., Van der Vorst, J., Flemming, R.J. and Parkins, D.C., "Icing Certification of Korean Utility Helicopter KUH-1: Artificial Icing Flight Test", presented at 9th AIAA Atmospheric and Space Environments Conference, USA, June 5-9, 2017.

2. Park, N.E., Woo, C.H., Kim, H.S., Kim K.S., et al., "A Study on the Test and Computational Simulation for the Design of Helicopter De/Anti-Icing System", presented at 7th Asian/Australian Rotorcraft Forum, South-Korea, October 30 – November 1, 2018.

3. De Bruin, A. C., Fatigani, G. and Shin, H. B., "KAI Surion Helicopter Full-Scale Air Intake Testing at CIRA Icing Wind Tunnel," presented at 30th Congress of International Council of the Aeronautical Sciences, Korea, September 25-30, 2016.

4. Lammers, K., Van 't Hoff, S.C., Ferschitz, H. and Wannemacher M., "Helicopter Engine Air Intake Icing Wind Tunnel Certification Test", presented at 44th European Rotorcraft Forum, The Netherlands, September 18-21, 2018.

5. Anderson, D.N., "Manual of Scaling Methods", NASA/CR-2004-212875, March, 2004.

6. Orchard, D.M., Addy, H.E., Wright, W.B. and Tsao, J., "Altitude Scaling of Thermal Ice Protection Systems in Running Wet Operation", National Research Council Canada, presented at the 9th AIAA Atmospheric and Space Environments Conference, USA, June 5-9, 2017.

7. Flemming, R.J., "The Past Twenty Years of Icing Research and Development at Sikorsky Aircraft", presented at the 40th AIAA Aerospace Sciences Meeting & Exhibit, USA, January 14-17, 2002.

8. Flemming, R.J., K.W. Hanks and M.L. Hanks, "US Army UH-60M Helicopter Main Rotor Ice Protection System", presented at SAE Aircraft & Engine Icing International Conference, Spain, September 24-27, 2007.

9. Jeck, R.K., "Icing Design Envelopes (14 CFR Part 25 and 29, Appendix C) Converted to a Distance-Based Format", DOT/FAA/AR-00/30, April, 2002.

10. Uiterlinden, R.M., Timmerman, B., Tuinstra M., et al., "Camera-Based Imaging Flight test Instrumentation", presented at 28th Society of Flight Test Engineers Symposium, Italy, September 12-15, 2017.

Dedicated to innovation in aerospace

Royal Netherlands Aerospace Centre

NLR is a leading international research centre for aerospace. Bolstered by its multidisciplinary expertise and unrivalled research facilities, NLR provides innovative and integral solutions for the complex challenges in the aerospace sector.

NLR's activities span the full spectrum of Research Development Test & Evaluation (RDT & E). Given NLR's specialist knowledge and facilities, companies turn to NLR for validation, verification, qualification, simulation and evaluation. NLR thereby bridges the gap between research and practical applications, while working for both government and industry at home and abroad.

NLR stands for practical and innovative solutions, technical expertise and a long-term design vision. This allows NLR's cutting edge technology to find its way into successful aerospace programs of OEMs, including Airbus, Embraer and Pilatus. NLR contributes to (military) programs, such as ESA's IXV re-entry vehicle, the F-35, the Apache helicopter, and European programs, including SESAR and Clean Sky 2.

Founded in 1919, and employing some 600 people, NLR achieved a turnover of 76 million euros in 2017, of which 81% derived from contract research, and the remaining from government funds.

For more information visit: **www.nlr.org**

Postal address
PO Box 90502
1006 BM Amsterdam, The Netherlands
e) info@nlr.nl **i)** www.nlr.org

NLR Amsterdam
Anthony Fokkerweg 2
1059 CM Amsterdam, The Netherlands
p) +31 88 511 3113

NLR Marknesse
Voorsterweg 31
8316 PR Marknesse, The Netherlands
p) +31 88 511 4444